Proteinticle Engineering for Accurate 3D Diagnosis

Jong-Hwan Lee,[†,||] Hyuk Seong Seo,[†,||] Jong Am Song,[†,||] Koo Chul Kwon,[†] Eun Jung Lee,[†] Ho Jin Kim,[‡] Eun Bong Lee,[§] Young Joo Cha,[⊥] and Jeewon Lee[†,*]

[†]Department of Chemical and Biological Engineering, College of Engineering, Korea University, Anam-Ro 145, Seoul 136-713, Republic of Korea, [‡]Department of Neurology, Research Institute and Hospital of National Cancer Center, 323 Ilsan Street, Ilsandong-gu, Goyang-si, Gyeonggi-do, Republic of Korea, [§]College of Medicine, Seoul National University, Daehak-Ro 103, Seoul 110-744, Republic of Korea, and [⊥]College of Medicine, Chung-Ang University, Heuksuk-Ro 84, Seoul 156-756, Republic of Korea. [||]J.-H. Lee, H. S. Seo, and J. A. Song contributed equally to this work.

ABSTRACT In nature certain proteins are self-assembled inside cells to form nanoscale particles (named "proteinticles") with constant structure and surface topology. Unlike chemically synthesized nanomaterials (*e.g.*, various metal, carbon, and polymer nanoparticles), a variety of functional proteinticles can be easily created through genetic modification of the proteinticle surface, *i.e.*, by adding or inserting specified proteins/peptides to the N- or C-terminus or the internal region of the protein constituent. Here we present proteins/peptides that recognize disease-specific antibodies on the surface of human ferritin based proteinticles for accurate 3D diagnosis of human autoimmune and infectious diseases. The surface display of the extracellular domain of myelin oligodendrocyte glycoprotein (MOG) with native conformation successfully discriminated between autoantibodies to native or denatured MOG, leading to the reliable diagnosis of multiple sclerosis with enhanced accuracy. Also we simultaneously displayed different antigenic peptides from hepatitis C virus (HCV) on the same proteinticle surface with modulating the composition of each peptide. The proteinticles with the heterogeneous peptide surface detected anti-HCV antibodies in patient sera with 100% accuracy. The proposed method of proteinticle engineering can be applied in general to the sensitive and specific diagnosis of many other human diseases.
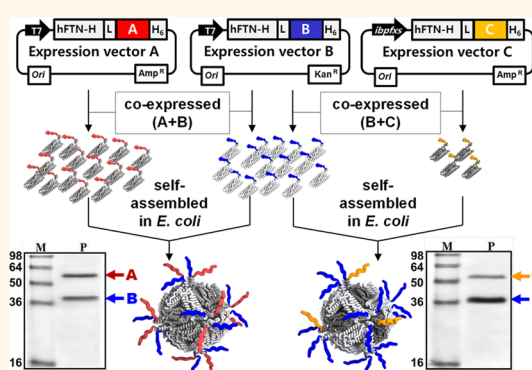
KEYWORDS: proteinticles · self-assembly · nanomaterials · surface engineering · 3D diagnosis

Autoantibodies against a native human antigen reflect the occurrence and severity of an autoimmune disease. Detection of the circulating autoantibodies at elevated concentration in patient serum is of crucial importance for diagnosis and treatment of autoimmune diseases as well as monitoring disease progression.[1] It is notable that in many autoimmune diseases (*e.g.*, rheumatoid arthritis, multiple sclerosis, systemic lupus erythematosus, Sjögren's syndrome, scleroderma, autoimmune hepatitis, *etc.*),[2,3] autoantibodies are also found in some healthy individuals, implying that positive signals from healthy sera should not be regarded simply as "false positive"; that is, they could be "true positive". In most cases of immunoassay, the signals from healthy controls are used to determine the cutoff value (COV), *i.e.*, the threshold to distinguish negative from positive signals, which is calculated according to the following IUPAC definition:[4] (average of negative control signals) + *n*(standard deviation),

where *n* is a numerical factor, chosen in accordance with the confidence level. The coexistence of both "true" and "false positive" signals can significantly increase the standard deviation of healthy control signals, and therefore COV varies widely depending on the chosen value of the numerical factor (*n*) as well as the number of healthy controls tested. When a higher COV is selected, the true negative fraction of healthy controls (specificity) will increase, while the true positive fraction of patients (sensitivity) will decrease. Therefore, the increased variability of COV makes it very difficult to diagnose autoimmune diseases with high accuracy and reliability. This is in part the reason that diagnostic performance of the same autoimmune disease has not been reproduced by different research groups, as presented in Supplementary Table S1, and remains controversial.

To solve this problem, we should minimize false positive signals from autoantibody-free healthy controls and make assay
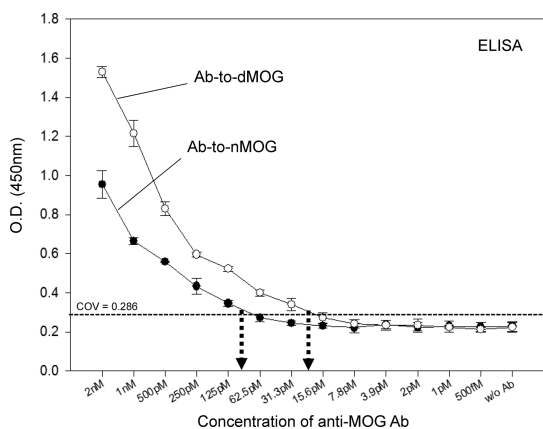
Figure 1. Results of ELISA-based detection of conformation-sensitive (●) and conformation-independent (○) anti-MOG antibodies.

sensitivity and specificity not significantly influenced by a particular decision threshold (COV). The previous studies[5−7] identified two different types of autoantibodies: one is conformation-sensitive autoantibodies against native protein, and the other one is conformation-independent autoantibodies that bind solely to denatured protein or short synthetic peptides. The latter one usually has nonspecific cross-reactivity with a linear peptide of irrelevant proteins and hence is responsible for the occurrence of false positive signals. Therefore, an effective, or probably the best way to eliminate false positive signals from healthy controls is to selectively detect antigen-specific and conformation-sensitive autoantibodies. Unfortunately, the conventional ELISA cannot discriminate the antibodies against native or denatured protein, as shown in Figure 1, presenting the results of detection of anti-human myelin oligodendrocyte glycoprotein (MOG) antibodies, a marker of multiple sclerosis (MS).

Unlike autoimmunity by native human antigen, viral infection causes severe immune responses to external viral antigen, which includes in general production of anti-virus polyclonal antibodies.[8] Since diagnosis of viral infection requires sensitive detection of polyclonal antibodies, various epitopes from viral antigens should be simultaneously used as capture probes, and the composition of each epitope and access of antibodies to well-oriented epitopes are also important. In traditional diagnosis of viral infection, antigenic eptiopes are chemically immobilized in a random fashion on a two-dimensional solid surface,[9,10] which causes significant problems such as uncontrolled orientation, clustering, inactivation, and/or instability of antigenic epitopes and hence decreases detection sensitivity. Here the proteinticles were also engineered to simultaneously display the different antigenic epitopes of HCV on the same proteinticle surface with modulating the epitope composition to minimize the "false negative" rate in the detection of anti-HCV polyclonal antibodies. HCV is a small enveloped virus containing

single-stranded positive sense RNA and is a major cause of chronic hepatitis, cirrhosis, and hepatocellular carcinoma. Worldwide more than 170 million people now suffer from hepatitis C, and more than 350 000 people die yearly from hepatitis C-related diseases. Although about 3 to 4 million people are newly infected every year,[8,11,12] there is no vaccine currently available for the prevention of HCV infection,[13] and therefore sensitive and early diagnosis is of crucial importance to bring hepatitis C under control. Although the diagnostic assays of MS and hepatitis C were demonstrated as proof-of-concept in this study, the proposed method of proteinticle engineering can be applied in general to the sensitive and specific diagnosis of many other human diseases.

RESULTS AND DISCUSSION

Diagnosis of Autoimmune Disease (MS) Using Proteinticles That Are Engineered to Display Human Antigens (MOG) with Native Conformation. Here we engineered human ferritin-based proteinticles to detect the conformation-sensitive autoantibodies against native human MOG. MS is the most common chronic neurological and autoimmune disease in Europe and North America[14] and was chosen in this study as a representative of autoimmune disease, because the anti-MOG antibodies are also found in healthy controls in common with many other autoimmune diseases. The IgV-like extracellular domain of MOG on the outermost myelin lamellae is exposed to the extracellular space,[15] which is easily accessible for autoantibodies and is presumed to have a conformational epitope recognized by the confirmation-sensitive autoantibodies. Each of the extracellular domain (G30 to G154) and short peptide (A61 to P92) of MOG was genetically fused to the C-terminus of human ferritin heavy chain (hFTN-H) *via* a linker sequence ($G_3SG_3TG_3SG_3$). Owing to the self-assembly activity of hFTN-H that forms homopolymer (24mer) in the spherical shape with a diameter of about 12 nm,[16,17] the modified hFTN-Hs were also self-assembled to form spherical proteinticles when expressed in *Escherichia coli* (Supplementary Figure S1). Each proteinticle displays 24 extracellular domains or 24 peptides on its surface, which is named here MOG-extra 24mer or MOG-peptide 24mer, respectively (Figure 2a). (MOG-peptide 24mers were prepared and used as a control to prove the advantage of MOG-extra 24mers.) Then the MOG-extra or MOG-peptide 24mers were distributed within a polyacrylamide-based porous hydrogel (Supplementary Figure S2) that is prepared by a simple copolymerization following covalent linkages between the proteinticles and acrylamide,[18] resulting in the formation of a 3D diagnostic platform. The anti-MOG antibodies that are captured by MOG-extra or MOG-peptide 24mers were finally detected by anti-human antibodies conjugated with quantum dot (CdSe), emitting fluorescence at 655 nm.
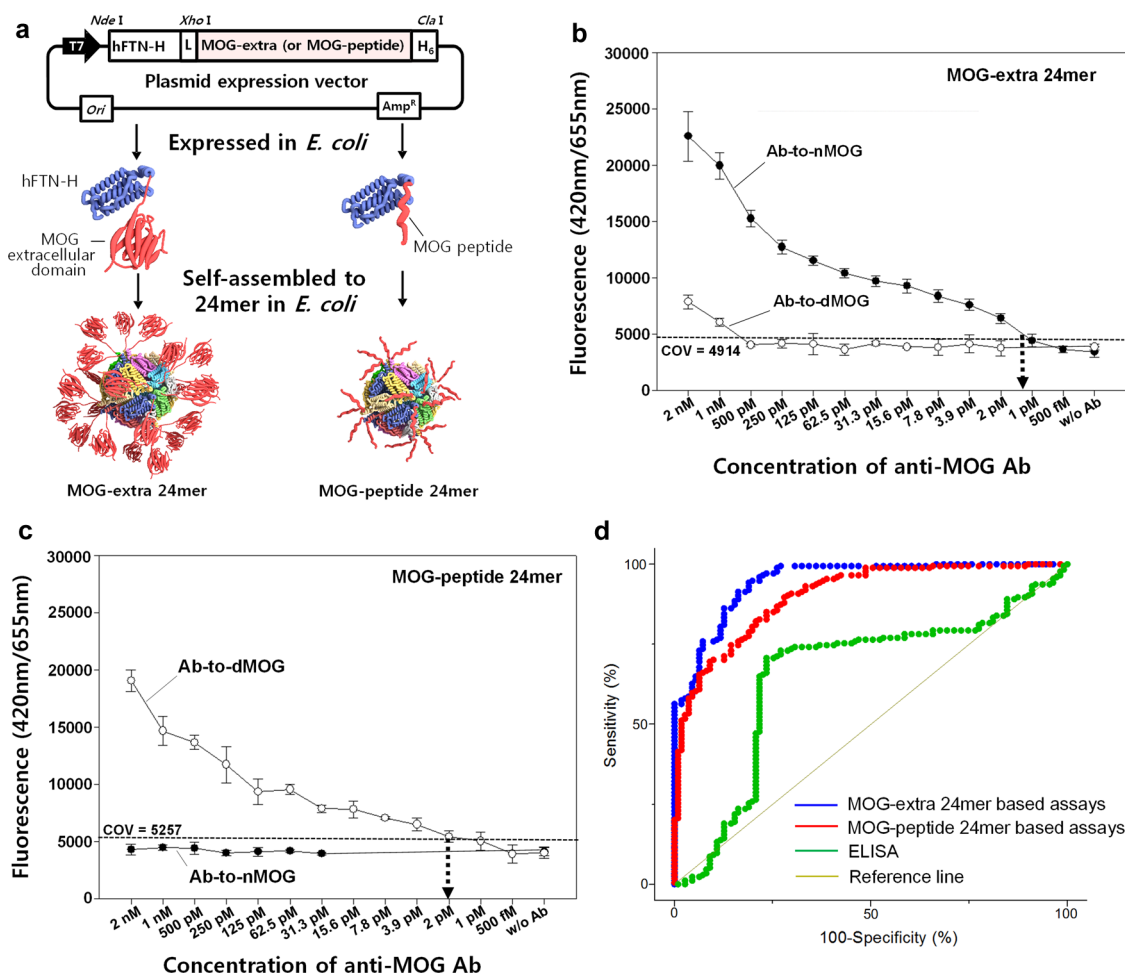
Figure 2. (a) Schematic showing the synthesis of proteinticle-based MOG-extra and MOG-peptide 24mers, where human ferritin heavy chain (hFTN-H) and MOG extracellular domain (or peptide) are represented by colorful wires and red ribbon, respectively. (L in plasmid expression vector represents linker sequence, $G_3SG_3TG_3SG_3$.) (b) Results of MOG-extra 24mer based detection of conformation-sensitive (●) and conformation-independent (○) anti-MOG antibodies. (c) Results of MOG-peptide 24mer based detection of conformation-sensitive (●) and conformation-independent (○) anti-MOG antibodies. (d) ROC curves showing the assay performance of MOG-extra and MOG-peptide 24mer based assays and ELISA in the diagnosis of MS.

The MOG-extra 24mers successfully distinguished the antibodies against native MOG (named Ab-to-nMOG) from those against synthetic MOG peptide (named Ab-to-dMOG) (Figure 2b), and the detectable minimum concentration of Ab-to-nMOG was significantly lowered to about 1 pM (indicated by a dotted arrow) compared to ELISA (Figure 1), indicating more sensitive detection. Figure 2b also shows that Ab-to-dMOG at a high concentration near 2 nM weakly interacts with MOG-extra 24mers, which however seems clinically insignificant because the actual concentration of anti-MOG antibodies in patient sera never reaches 2 nM (Supplementary Table S2, showing that in 96% of 50 MS patient sera, anti-MOG antibody concentration was lower than 1.5 nM). From Figure 2c, it is evident that MOG-peptide 24mers never detected Ab-to-nMOG. Consequently, Ab-to-nMOG was detected only by MOG-extra 24mers, indicating that the native conformation of MOG-extra was correctly formed on the proteinticle surface.

Fifty MS patient and 37 healthy sera were tested using the MOG-extra and MOG-peptide 24mers, using ELISA-negative healthy controls as negative controls. When analyzed with variation in COV (Supplementary Tables S3, S4 and Figure S3), the test results show that the MOG-extra 24mer based assays have the least dependence of sensitivity and specificity on COV, implying the most reliable assay. (All the assay results are presented and discussed in detail in the Supporting Information.) The assay performance of proteinticle-based assays and ELISA was evaluated through the analysis of the receiver operating characteristic (ROC) curve,[19] plotting the true positive rate [sensitivity (%)] as a function of the false positive rate [100 − specificity (%)] for every possible COV (Figure 2d). Each point of the ROC curve represents a sensitivity−specificity pair that is estimated using a particular COV. The closer the ROC curve is to upper left corner (100% sensitivity and 100% specificity, representing perfect discrimination), the higher the assay accuracy is. It is evident from

Figure 2d that the MOG-extra 24mer based detection of conformation-sensitive autoantibodies is the most accurate and reliable diagnostic method for MS.

In conventional ELISA, protein probes are randomly immobilized on a 2D solid surface that is already chemically activated, and the native conformation of protein probes is mostly altered or often completely lost on the chemically modified surface. This is the reason that traditional ELISA cannot discriminate between conformation-sensitive and conformation-independent antibodies (Figure 1). Moreover, the orientation of protein probes is also uncontrollable upon random immobilization (Supplementary Figure S4), and thereby only a limited fraction of the randomly oriented protein probes are allowed to capture target analytes in the test sample, leading to a significant decrease in sensitivity. On the other hand, proteinticles provide a 3D biological surface where protein probes can be biologically displayed with native conformation and be well oriented, leading to selective detection of conformation-sensitive antibodies. Also, peptide probes are displayed with homogeneous and correct orientation on the engineered proteinticle surface, resulting in the higher sensitivity of MOG-peptide 24mer based assays compared to ELISA (Supplementary Table S5). The superiority of proteinticle-based assays over ELISA is described in detail as well in our previous reports.[18,20−22] This advantage of proteinticles is of crucial importance to basic immunology research to study the role of conformation-sensitive autoantibodies in pathogenesis or disease progression of many autoimmune diseases (*e.g.*, rheumatoid arthritis, multiple sclerosis, systemic lupus erythematosus, Sjögren's syndrome, scleroderma, autoimmune hepatitis, *etc.*), which remains currently unresolved.[15] Also in this study, we immobilized proteinticles within a porous hydrogel, resulting in a highly sensitive 3D bioassay through combining 3D proteinticles with 3D porosity of the hydrogel, which provides an enlarged surface area (Supplementary Figure S5). Also the moisture-rich environment of the hydrogel allows the bioactivity of proteinticles to be stably maintained during a prolonged period.

Diagnosis of Infectious Disease (Hepatitis C) Using Proteinticles That Are Engineered to Display Multiple and Different Viral Antigens (HCV). We also engineered human ferritin-based proteinticles to sensitively detect the antibodies against structural and nonstructural proteins of hepatitis C virus (HCV). The HCV genome encodes three structural proteins (core, E1, and E2) and five nonstructural proteins (NS1, NS2, NS3, NS4, and NS5). Here we selected the following three epitopes recognized by anti-HCV antibodies: epitope A (EA) (K10 to S53) in core protein, epitope B (EB) (A1192 to C1457) in NS3 protein, and epitope C (EC) [(I1694 to L1735)−(I1920 to V1935)] in NS4 protein.

First, each epitope of EA, EB, and EC was displayed on the proteinticle surface (Figure 3a), resulting in a "mono-epitope" display on the proteinticle. When each of EA-, EB-, and EC-proteinticles (Supplementary Figure S6) was tested in the diagnosis of 30 hepatitis C patients with 30 healthy controls, the highest sensitivity (90%) was achieved with EB-proteinticle; however false negative signals occurred for three patient sera (Figure 3b). It seems that EA, EB, and EC need to be used together to eliminate the false negative signals. The mixing of three different proteinticles may be a simple solution, but it requires a tedious synthesis and purification process per proteinticle. Instead, we tried to display all the epitopes on the same proteinticle using a two-vector-based coexpression system in recombinant *E. coli* (Figure 3a,c, Supplementary Figure S6), resulting in a "multi-epitope" display on the proteinticle. Figure 3a, c, and d show that even the surface composition of each epitope can be modulated using the difference in promoter strength. Compared to the strong T7 promoter, *ibpfxs*[23] is the σ^{32}-dependent weak and hybrid promoter that is synthesized by tandem linking the promoters from *ibpAB* and *fxs*A encoding two small heat shock proteins (IbpA and IbpB) and inner membrane protein (FxsA), respectively. Reportedly,[23] the overproduction of recombinant protein induces a heat shock-like response and σ^{32}-regulon. The time-course monitoring of recombinant protein expression (Figure 3d) shows that the promoter *ibpfxs* gets turned on weakly after the T7-induced recombinant protein synthesis begins in *E. coli* and that the fraction of EB or EC−EA (tandem linked epitope) on the proteinticle surface is always nearly constant, indicating the surface fraction of different epitopes depends on promoter strength, not significantly influenced by duration time of gene expression. The proteinticles with the heterogeneous surface that displays both EB and EC−EA enhanced the assay performance, and finally 100% sensitivity was achieved when the surface fraction of EB increased to 80% on the proteinticle surface (Figure 3b), which exactly corresponds to the results of the ROC curve analysis (Figure 3e). When the mixture of synthetic peptide epitopes [EB (80%) and EC−EA (20%)] was directly immobilized on the 2D surface of a 96-well plate (Costar high binding black polystyrene 96-well plate, Corning Inc., Corning, NY, USA), assay sensitivity was only 63% (Supplementary Figure S7), indicating that the proteinticle-based 3D assay is much more accurate.

The immunoassay of viral infection requires sensitive and reliable detection of anti-virus polyclonal antibodies, for which multiple and different epitopes from a viral antigen should be simultaneously used to detect polyclonal antibodies. The simple mixing of different epitopes followed by random immobilization on a 2D surface causes the same problems (uncontrolled orientation, denaturation of native conformation, *etc.*) as ELISA. An effective solution to solve the problems is to simultaneously display multiple and different epitopes on the biological surface of a proteinticle, which enables
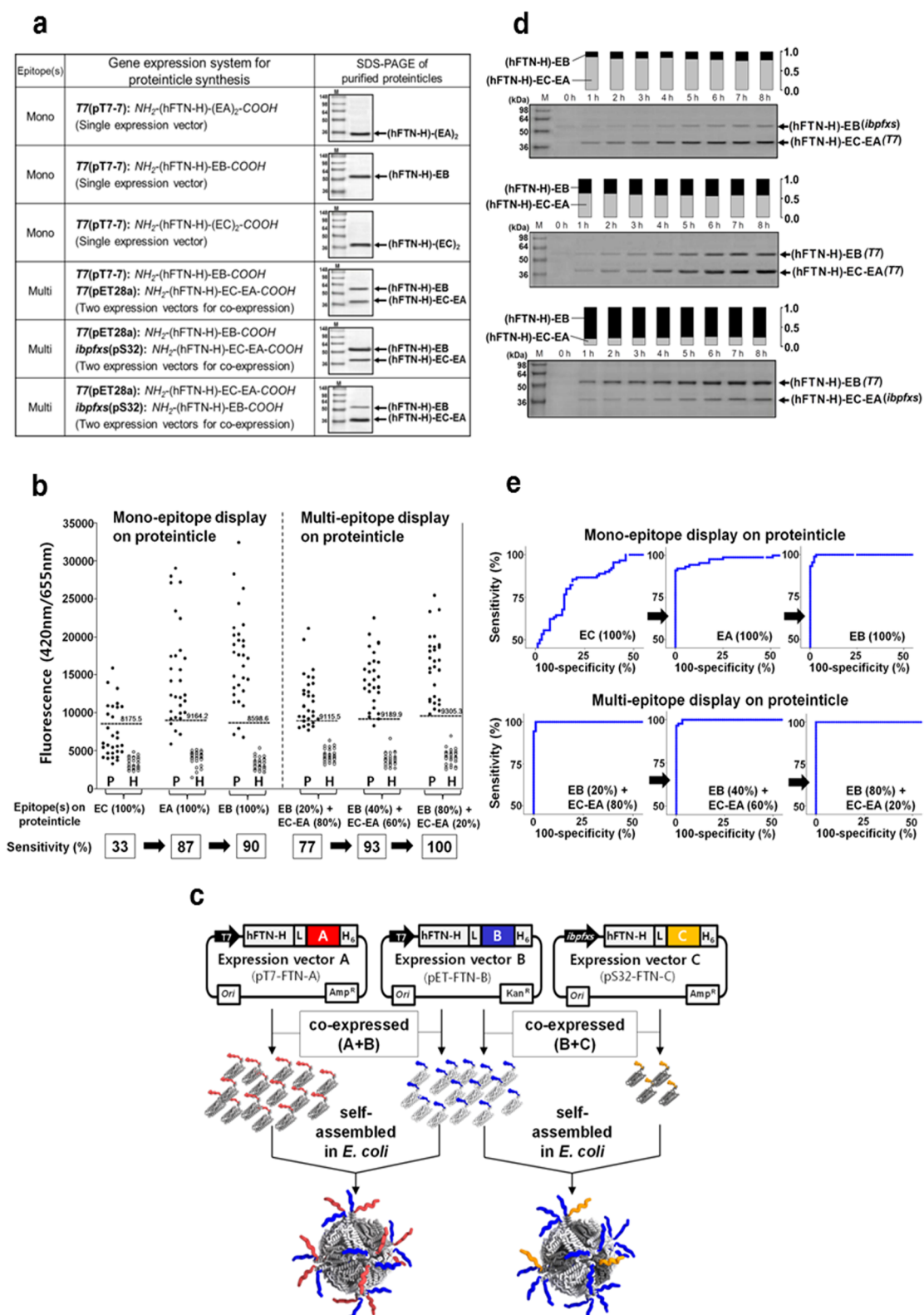
Figure 3. (a) *E. coli* gene expression systems used for mono- and multi-epitope display on the hFTN-H based proteinticles and SDS-PAGE of synthesized and purified proteinticles (pT7-7, pET28a, and pS32 represent plasmid expression vectors used). (b) Results of proteinticle-based diagnosis of hepatitis C and sensitivity analysis (P and H represent patients and healthy individuals, respectively). (c) Two-vector-based coexpression systems used in *E. coli* to synthesize the proteinticles that display multiple and different epitopes together (A+B or B+C) with modulating the surface fraction of each epitope (L in expression vectors represents linker sequence, $G_3SG_3TG_3SG_3$). (d) Time-course analysis of SDS-PAGE of the proteinticles expressed by the coexpression system in *E. coli*. [Bar graphs indicate time-course variation in the fraction of each protein component, (hFTN-H)-EB or (hFTN-H)-EC−EA, that a proteinticle comprises.] (e) ROC curves showing the assay performance of proteinticle-based diagnosis of hepatitis C.

the displayed epitopes to have homogeneous orientation and conformation on the proteinticle surface and hence makes antibody detection reproducible and reliable. Here we were even able to modulate quantitative composition of each epitope on the proteinticle surface using a two-vector-based coexpression system that employs two promoters with different strengths (Figure 3c), which can provide an effective method to rapidly identify active epitopes of viral antigen and furthermore an optimum composition of the epitopes to detect polyclonal antibodies with 100% accuracy.

CONCLUSIONS

Recently, synthetic inorganic and organic nanomaterials (*e.g.*, various metal, carbon, and polymer nanoparticles) have been extensively studied for bioassays to overcome the sensitivity limit of ELISA. Synthetic nanomaterials have important properties such as large surface to volume ratio, a variety of physical and chemically tailorable properties, and overall structural robustness. However, an inevitable drawback of synthetic nanomaterials used for biological application is that they intrinsically lack bioactivity. Prior to being used for bioassays, the synthesized nanomaterials should be biologically functionalized by attaching active biomolecules on the chemically modified surface of nanomaterials; however, surface composition, density, orientation, and conformation of biomolecules are not controllable at all due to the random chemical attachment (Supplementary Figure S8), indicating that conventional ELISA-associated problems remain still unsolved. Moreover, there is a serious concern about potential safety problems of synthetic nanomaterials. That is, despite the progress in research of diverse synthetic nanomaterials, even developers and regulators remain uncertain about their associated risks[24] in environmental, health, and safety aspects.

Unlike the synthetic nanomaterials above, proteinticles are biological nanoparticles that are naturally self-assembled inside cells and hence never cause nanotoxicity such as potential long-term accumulation in human organs/tissues. Also, through simple genetic modification, the proteinticle surface can be engineered to have a variety of special functions. Here we displayed native human and viral antigens on a ferritin-based proteinticle surface, which successfully reduced "false positive" and "false negative" rates in the diagnosis of autoimmune disease and viral infection, respectively. On the basis of significant advantages of proteinticles that are evidenced in this study, it seems that proteinticles and proteinticle engineering can shift the current paradigm of nanotechnolgy research that depends on chemically synthesized and artificial nanomaterials to the research based on biologically synthesized and natural nanomaterials, *i.e.*, proteinticles. Although the diagnostic assays of MS and hepatitis C were demonstrated as proof-of-concept in this study, the proposed method of proteinticle engineering can be used to solve crucial problems of traditional bioassays based on antigen–antibody interaction and be applied in general to sensitive and specific diagnosis of many other human diseases.

METHODS

Engineering and Biosynthesis of Proteinticles Used for the Diagnosis of MS. Through PCR amplification using the appropriate primers, four gene clones were prepared, encoding *N*-NdeI-(hFTN-H)-$G_3SG_3TG_3SG_3$(linker)-*Xho*I-*C*, *N*-*Xho*I-MOG extracellular domain (G30-G154)-H_6-*Cla*I-*C*, and *N*-*Xho*I-MOG peptide [(A61-P92)$_2$]-H_6-*Cla*I-*C*. The hFTN-H gene was cloned using the previously prepared expression vector, and the genes encoding extracellular domain and peptide of MOG were cloned through assembly PCR. Each gene clone was sequentially ligated into pT7-7 plasmid to construct the expression vector pT7-hFTN-MOG-Ex and pT7-hFTN-MOG-Pep, coding for the synthesis of *N*-(hFTN-H)-linker-(MOG-extracellular domain)-H_6-*C* and *N*-(hFTN-H)-linker-(tandem sequence of MOG-peptide)-H_6-*C*, respectively. After complete sequencing, *E. coli* Origami(DE3) was transformed with the above expression vectors, and both kanamycin- and ampicillin-resistant transformants were finally selected. The detailed procedures for recombinant gene expression, recombinant protein purification, and TEM image analysis are well described in our previous report.[25] The hydrodynamic diameter of the proteinticle was determined by dynamic light scattering (DLS) using a zeta potential/particle sizer (Brookhaven Instruments, NY, USA), after the proteinticles were well dispersed in PBS buffer (137 mM NaCl, 2.7 mM KCl, 10 mM Na_2HPO_4, 2 mM KH_2PO_4, pH 7.4).

Engineering and Biosynthesis of Proteinticles Used for the Diagnosis of Hepatitis C. Through PCR amplification using the appropriate primers, five gene clones were prepared, encoding *N*-NdeI-(hFTN-H)-$G_3SG_3TG_3SG_3$(linker)-*Xho*I-*C*, *N*-*Xho*I-(K10-S53)$_2$-H_6-*Hind*III-*C*, *N*-*Xho*I-(A1192-C1457)-H_6-*Hind*III-*C*, *N*-*Xho*I-[(I1694-L1735)-$G_3SG_3TG_3SG_3$-(I1920-V1935)]$_2$-H_6-*Hind*III-*C*, and *N*-*Xho*I-(I1694-L1735)-$G_3SG_3TG_3SG_3$-(I1920-V1935)-(K10-S53)-*Hind*III-*C*, where the sequences above, K10-S53, A1192-C1457, I1694-L1735, and I1920-V1935, are from structural and nonstructural proteins of HCV and were cloned through assembly PCR. Each gene clone was sequentially ligated into pT7-7, pET28a, or p32 plasmid to construct the expression vectors pT7-FTN-EA, pT7-FTN-EB, pT7-FTN-EC, pET-FTN-EB, pET-FTN-ECA, p32-FTN-EB, and p32-FTN-ECA, coding for the synthesis of *N*-(hFTN-H)-linker-(EA)$_2$-H_6-*C*, *N*-(hFTN-H)-linker-EB-H_6-*C*, *N*-(hFTN-H)-linker-(EC)$_2$-H_6-*C*, and *N*-(hFTN-H)-linker-EC-EA-*C*, where the HCV epitopes EA, EB, and EC correspond to K10-S53, A1192-C1457, and (I1694-L1735)-$G_3SG_3TG_3SG_3$-(I1920-V1935), respectively. After complete sequencing, *E. coli* BL21(DE3) was transformed with one of the expression vectors pT7-FTN-EA, pT7-FTN-EB, and pT7-FTN-EC, and ampicillin-resistant transformants were finally selected and used to synthesize the proteinticles with mono-epitope display. To synthesize the proteinticles with multi-epitope display, *E. coli* BL21(DE3) was cotransformed by a pair of recombinant expression vectors, that is, pT7-FTN-EB and pET-FTN-ECA, p32-FTN-EB and pET-FTN-ECA, or pET-FTN-EB and p32-FTN-ECA, and both kanamycin- and ampicillin-resistant transformants were selected. The detailed procedures for recombinant gene expression and recombinant purification are well described in our previous report.[25]

Preparation of Proteinticle-Embedded Hydrogel. Proteinticles were modified by *N*-succinimidyl-acrylate (NSA, 0.01 mg) in PBS buffer (137 mM NaCl, 2.7 mM KCl, 10 mM Na_2HPO_4, 2 mM KH_2PO_4, pH 7.4) for 1 h at 37 °C, resulting in the synthesis of vinylated proteinticles. Unreacted NSA was eliminated by ultrafiltration (Amicon Ultra 100K, Millipore, Billerica, MA, USA).

Proteinticle-embedded hydrogel was prepared through the reaction with 30 μg of the vinylated proteinticle, 9% acrylamide (29:1 w/w acrylamide/bis-acrylamide), and 0.125% w/v ammonium persulfate. Immediately after the addition of 0.125% v/v tetramethylethylenediamine, 50 μL of the reaction mixture above was immediately loaded into a Nunc Delta black 96-well plate (Nunc, Roskide, Denmark) and copolymerized for 16 h at 25 °C. A more detailed procedure to prepare the hydrogel is well described in our previous report.[18] The morphology of the hydrogel was analyzed by a field emission scanning electron microscope (Hitach S-4700, Japan). Prior to SEM analysis, the hydrogel was shock-frozen in liquid nitrogen, quickly transferred to a freeze drier (FDU-2100, DRC-1000, EYELA, Japan), and lyophilized for 6 h. The surface of the hydrogel was coated by platinum before SEM observation.

MOG-Extra and MOG-Peptide 24mer Based Detection of Conformation-Sensitive and Conformation-Independent Anti-MOG Antibodies. The standard anti-MOG antibodies [goat anti-MOG polyclonal antibody, which reacts only with native human MOG (*i.e.*, conformation-sensitive antibodies) (Abgent Inc., San Diego, CA, USA), and rabbit anti-MOG polyclonal antibody, which reacts with the N-terminal end of human MOG (*i.e.*, conformation-independent antibodies) (Abcam, Cambridge, UK)] were used as target analytes to be detected by MOG-extra and MOG-peptide 24mers, and the results were compared with ELISA (AnaSpec Inc., Fremont, CA, USA). Q-dot (CdSe)-conjugated anti-goat(or rabbit) antibodies [1 nM, Qdot 655-rabbit F(ab')$_2$ anti-goat IgG conjugate and Qdot 655-goat F(ab')$_2$ anti-rabbit IgG conjugate (Invitrogen, Carlsbad, CA, USA)] were used as secondary/reporter antibodies. After rinsing with PBS buffer, each hydrogel [*i.e.*, MOG-extra (or MOG-peptide) 24mer-embedded hydrogel] was used to detect the standard anti-MOG antibodies above at various concentrations (100 μL) through incubation with slow agitation for 2 h at room temperature. After a sufficient washing step with PBS buffer, 100 μL of Q-dot conjugated anti-goat-(or rabbit) secondary antibodies (1 nM) was added, incubated with slow agitation for 1 h at room temperature, and finally washed again with PBS buffer. Then fluorescence was measured using a microplate reader (Infinite M200 PRO, TECAN, Austria) with excitation and emission at 420 and 655 nm, respectively. In the MOG-extra (or MOG-peptide) 24mer based assays, the cutoff-value was determined by the mean fluorescence signal of the negative control (PBS only) plus 3-fold standard deviation. The ELISA-based detection assays were performed according to the supplier's instruction: a standard curve (absorbance at 450 nm *vs* standard antibody concentration) was first prepared, and the absorbance value corresponding to zero antibody concentration was used as COV. All the assay results were presented with error bars based on the results of triplicate experiments.

Diagnostic Assays of MS and Hepatitis C with Patients and Healthy Controls. The human sera of 50 MS patients and 37 healthy controls were kindly donated by the Research Institute and Hospital of National Cancer Center at Korea. All the diagnostic assays were performed using the same MOG-extra (or MOG-peptide) 24mer-embedded hydrogel in a Nunc Delta black 96-well plate (Nunc, Roskide, Denmark). After rinsing with PBS buffer, the MS patient or healthy serum (100 μL) that was already 100-times diluted with PBS buffer were added to each hydrogel, followed by incubation with slow agitation for 2 h at room temperature. After a sufficient washing step with PBS buffer, 100 μL of Q-dot-conjugated anti-human secondary antibodies [1 nM, Qdot 655-goat F(ab')$_2$ anti-human IgG conjugate (Invitrogen, Carlsbad, CA, USA)] was added, incubated with slow agitation for 1 h at room temperature, and finally washed sufficiently with PBS buffer. Then fluorescence was measured using a microplate reader (Infinite M200 PRO, TECAN, Austria) with excitation and emission at 420 and 655 nm, respectively. Also, the commercial ELISA kit (AnaSpec Inc., Fremont, CA, USA) for MS diagnosis was used according to the supplier's instructions. All the assay results were presented with error bars based on the results of triplicate experiments.

For the diagnosis of hepatitis C, the human sera of 30 hepatitis C patients and 30 healthy controls were kindly donated by the Seoul National University Hospital and the Human Serum Bank of Korea at Chungang University Medical Center. All the diagnostic assays were performed using the proteinticles with mono(either EA, EB, or EC)- or multi(all of EA, EB, and EC)-epitope display, which are also embedded within the hydrogel that is prepared in a Nunc Delta black 96-well plate (Nunc, Roskide, Denmark). The diagnostic procedure was exactly the same as described above for the MS diagnosis. For the diagnosis of hepatitis C using the epitope peptides only without proteinticles, 5 μg of the epitope peptide mixture (EB 80% and EC−EA 20%) in PBS buffer was directly immobilized on a conventional 96-well plate (Costar high binding black polystyrene 96-well plate, Corning Inc., Corning, NY, USA) through incubation for 12 h at 4 °C. After rinsing twice with PBS buffer, a 2 h blocking step was followed using 200 μL of Superblocker (Thermo Scientific, Rockford, IL, USA) at room temperature. Then 100 μL of 100-times diluted sera of hepatitis C patient and healthy controls in PBS buffer was added, followed by incubation at room temperature for 1 h. After the five consecutive washing steps using PBS buffer, 100 μL of Q-dot-conjugated anti-human secondary antibody [1 nM, Qdot 655-goat F(ab')$_2$ anti-human IgG conjugate (Invitrogen, Carlsbad, CA, USA)] was added, incubated for 1 h at room temperature, and sufficiently washed with PBS buffer. Fluorescence was measured using a microplate reader (Infinite M200 PRO, TECAN, Austria) with excitation and emission at 420 and 655 nm, respectively.

Conflict of Interest: The authors declare no competing financial interest.

Supporting Information Available: Supporting Information (additional discussion about MS diagnosis and supplementary figures and tables) is available free of charge *via* the Internet at http://pubs.acs.org.

REFERENCES AND NOTES

1. Leslie, D.; Lipsky, P.; Notkins, A. L. Autoantibodies as Predictors of Disease. *J. Clin. Invest.* **2001**, *108*, 1417–1422.
2. Arthur, K.; Russell, T.; John, R.; Daniel, H. S.; Henry, A. H. Guidelines for Clinical Use of the Antinuclear Antibody Test and Tests for Specific Autoantibodies to Nuclear Antigens. American College of Pathologists. *Arch. Pathol. Lab. Med.* **2000**, *124*, 71–81.
3. Malleson, P. N.; Mackinnon, M. J.; Sailer-Hoeck, M.; Spencer, C. H. Review for the Generalist: The Antinuclear Antibody Test in Children - When to Use It and What to Do with a Positive Titer. *Pediatr. Rheumatol. Online J.* **2010**, 10.1186/1546-0096-8-27.
4. Long, G. L.; Winefordner, J. D. Limit of Detection: A Closer Look at the IUPAC Definition. *Anal. Chem.* **1983**, *55*, 712A–724A.
5. Kobayashi, T.; Tanaka, S.; Okubo, M.; Nakanishi, K.; Murase, T.; Lernmark, A. Unique Epitopes of Glutamic Acid Decarboxylase Autoantibodies in Slowly Progressive Type 1 Diabetes. *J. Clin. Endocr. Metab.* **2003**, *88*, 4768–4775.
6. Hacker, M. K.; Janson, M.; Fairley, J. A.; Lin, M. S. Isotypes and Antigenic Profiles of *Pemphigus foliaceus* and *Pemphigus vulgaris* Autoantibodies. *Clin. Immunol.* **2002**, *105*, 64–74.
7. O'Connor, K. C.; McLaughlin, K. A.; De Jager, P. L.; Chitnis, T.; Bettelli, E.; Xu, C.; Robinson, W. H.; Cherry, S. V.; Bar-Or, A.; Banwell, B.; *et al.* Self-Antigen Tetramers Discriminate between Myelin Autoantibodies to Native or Denatured Protein. *Nat. Med.* **2007**, *13*, 211–217.
8. Bartosch, B.; Bukh, J.; Meunier, J. C.; Granier, C.; Engle, R. E.; Blackwelder, W. C.; Emerson, S. U.; Cosset, F. L.; Purcell, R. H. *In-Vitro* Assay for Neutralizing Antibody to Hepatitis C Virus: Evidence for Broadly Conserved Neutralization Epitopes. *Proc. Natl. Acad. Sci.* **2003**, *100*, 14199–14204.
9. Dufour, D. R.; Talastas, M.; Fernandez, M. D.; Harris, B.; Strader, D. B.; Seeff, L. B. Low-Positive Anti-Hepatitis C Virus

Enzyme Immunoassay Results: An Important Predictor of Low Likelihood of Hepatitis C Infection. *Clin. Chem.* **2003**, *49*, 479–486.

10. Thio, C. L.; Nolt, K. R.; Astemborski, J.; Vlahov, D.; Nelson, K. E.; Thomas, D. L. Screening for Hepatitis C Virus in Human Immunodeficiency Virus-Infected Individuals. *J. Clin. Microbiol.* **2000**, *38*, 575–577.

11. Ozaras, R.; Tahan, V. Acute Hepatitis C: Prevention and Treatment. *Expert. Rev. Anti.-Infect. Ther.* **2009**, *7*, 351–361.

12. Wilkins, T.; Malcolm, J. K.; Raina, D.; Schade, R. R. Hepatitis C: Diagnosis and Treatment. *Am. Fam. Physician* **2010**, *81*, 1351–1357.

13. Zhang, P.; Wu, C. G.; Mihalik, K.; Virata-Theimer, M. L.; Yu, M. Y.; Alter, H. J.; Feinstone, S. M. Hepatitis C Virus Epitope-Specific Neutralizing Antibodies in Igs Prepared from Human Plasma. *Proc. Natl. Acad. Sci.* **2007**, *104*, 8449–8454.

14. Steinman, L. Multiple Sclerosis: A Two-Stage Disease. *Nat. Immunol.* **2001**, *2*, 762–764.

15. von Büdingen, H. C.; Tanuma, N.; Villoslada, P.; Ouallet, J. C.; Hauser, S. L.; Genain, C. P. Immune Responses against the Myelin Oligodendrocyte Glycoprotein in Experimental Autoimmune Demyelination. *J. Clin. Immunol.* **2001**, *21*, 155–170.

16. Hempstead, P. D.; Yewdall, S. J.; Fernie, A. R.; Lawson, D. M.; Artymiuk, P. J.; Rice, D. W.; Ford, G. C.; Harrison, P. M. Comparison of the Three-Dimensional Structures of Recombinant Human H and Horse L Ferritins at High Resolution. *J. Mol. Biol.* **1997**, *268*, 424–448.

17. Luzzago, A.; Cesareni, G. Isolation of Point Mutations that Affect the Folding of the H Chain of Human Ferritin in *E. coli*. *EMBO J.* **1989**, *8*, 569–576.

18. Lee, E. J.; Ahn, K. Y.; Lee, J. H.; Park, J. S.; Song, J. A.; Sim, S. J.; Lee, E. B.; Cha, Y. J.; Lee, J. A Novel Bioassay Platform Using Ferritin-Based Nanoprobe Hydrogel. *Adv. Mater.* **2012**, *24*, 4739–4744.

19. Zweig, M. H.; Campbell, G. Receiver-Operating Characteristic (ROC) Plots: A Fundamental Evaluation Tool in Clinical Medicine. *Clin. Chem.* **1993**, *39*, 561–577.

20. Park, J.-S.; Cho, M.-K.; Lee, E. J.; Ahn, K.-Y.; Lee, K. E.; Jung, J. H.; Cho, Y.; Han, S.-S.; Kim, Y. K.; Lee, J. A Highly Sensitive and Selective Diagnostic Assay Based on Virus Nanoparticles. *Nat. Nanotechnol.* **2009**, *4*, 259–264.

21. Lee, J.-H.; Kim, J. S.; Park, J.-S.; Lee, W.; Lee, K. E.; Han, S.-S.; Lee, K. B.; Lee, J. A Three-Dimensional and Sensitive Bioassay Based on Nanostructured Quartz Combined with Viral Nanoparticles. *Adv. Funct. Mater.* **2010**, *20*, 2004–2009.

22. Lee, S. H.; Lee, H.; Park, J.-S.; Choi, H.; Han, K. Y.; Seo, H. S.; Ahn, K. Y.; Han, S.-S.; Cho, Y.; Lee, K. H.; *et al*. J. A Novel Approach to Ultrasensitive Diagnosis Using Supramolecular Protein Nanoparticles. *FASEB J.* **2007**, *21*, 1324–1334.

23. Kraft, M.; Knüpfer, U.; Wenderoth, R.; Pietschmann, P.; Hock, B.; Horn, U. An Online Monitoring System Based on a Synthetic Sigma32-Dependent Tandem Promoter for Visualization of Insoluble Proteins in the Cytoplasm of *Escherichia coli*. *Appl. Microbiol. Biotechnol.* **2007**, *75*, 397–406.

24. National Research Council. *A Research Strategy for Environmental, Health, and Safety Aspects of Engineered Nanomaterials*; The National Academies Press: Washington, DC, 2012.

25. Ahn, J. Y.; Choi, H.; Kim, Y. H.; Han, K. Y.; Park, J. S.; Han, S. S.; Lee, J. Heterologous Gene Expression Using Self-Assembled Supra-Molecules with High Affinity for HSP70 Chaperone. *Nucleic Acids Res.* **2005**, *33*, 3751–3762.